# Transistor Oscillators with Impedance Noise Matching

Günter Braun, *Member, IEEE*, and Heinz Lindenmeier, *Member, IEEE*

*Abstract*—**In the past noise optimization of HF and microwave transistor oscillators has usually been achieved experimentally. In this work a theory is derived which makes it possible to predict the carrier-to-noise ratio of a transistor oscillator with real components depending on parameters of the active element and the oscillator circuit which can be easily measured. The theory leads to new aspects of low-noise oscillator design which include the use of a multiple-stage active element and an impedance condition for noise matching. In this context the conditions for the use of GaAs FET's in low-noise oscillators are investigated. A consequent application of this theory in the design of oscillators can improve the carrier-to-noise ratio substantially. According to examples shown in this paper, an improvement of more than 50 dB may be reached over a nonoptimized oscillator. A verification by measurement has been made for seven single-transistor oscillators around 150 MHz. The measured values of the carrier-to-noise ratio show very good agreement with the values derived from theory. The differences between measured and calculated values are smaller than the measurement uncertainty of 3 dB.**

## I. Introduction

SINCE the introduction of a nonlinear amplitude control characteristic into oscillator theory by Van der Pol [1] in 1920, an increasing number of papers have been presented on the theory of oscillator operation. In parallel many papers have been published on the amplitude and frequency stability of oscillators. The few early publications on oscillator noise are mainly theoretical and describe basic properties of the noise of feedback systems. For example, Spälti [2] investigates the FM noise spectrum of a feedback tube oscillator, and Mullen [3] derives the spectral density of AM and FM noise of arbitrary LC oscillators with a Van der Pol control characteristic.

During the 1960's and 1970's, research on oscillator noise was concentrated on the noise properties of diode oscillators, while the advancing development of bipolar transistors with high power and transit frequency allowed their increasing application in HF and microwave oscillators. The noise optimization of transistor oscillators, however, was mainly achieved experimentally, with good noise properties often being obtained. Finally Leeson [4] described the oscillator noise by an empirically determined theory that requires an estimation of the "noise figure" of the active element.

Important breakthroughs in the calculation of transistor oscillator noise were achieved by Lindenmeier [5], [6] in 1974 and 1980. His calculations are based on a generally applicable derivation of spectral densities of AM and FM noise [5] similar to that of Mullen [3] but without Mullen's confinement to a Van der Pol control characteristic. The noise sources of a transistor which is fed back via an ideal transformer are transformed into a lossy parallel resonant circuit. In this way a calculation of carrier-to-noise ratio becomes possible, depending only on parameters of the active element and the oscillator circuit [6].

In this work the oscillator noise theory derived in [5] and [6] is extended to oscillators with real components. The resulting possibility of predicting the carrier-to-noise ratio depending only on transistor and circuit parameters is verified experimentally with seven different single-bipolar-transistor oscillators in the frequency range around 150 MHz. Their circuit parameters are selected such that the impact of every parameter on the carrier-to-noise ratio can be independently verified by measurement. A consequent noise optimization of these oscillators is deliberately not performed to permit more accurate measurements. Their carrier-to-noise ratios are in the range of $-90$ to $-110$ dBc for a frequency deviation from the carrier of 10 kHz.

The differences between calculated and measured values of the carrier-to-noise ratio are smaller than the measurement uncertainty of less than 3 dB, while a dynamic range of the test setup of more than 140 dB, related to 1 Hz bandwidth, is reached [7].

## II. Basic Theory

For a theoretical study of oscillator noise, a simple equivalent circuit of the oscillator is chosen. According to Mullen [3] and Lindenmeier [5], a comprehensive description of oscillator noise is possible with the noise equivalent circuit of Fig. 1.

The effective resonant circuit elements $L$ and $C$ represent the circuit inductance and capacitance including parasitic reactances in the circuit. Capacitances of the transistor which have influence on the resonant frequency of the circuit are also included in the value of $C$. The value

Manuscript received November 28, 1989; revised April 22, 1991.

G. Braun is with MBB Space Communications and Propulsion Systems, D-8000 Munich 80, Germany.

H. Lindenmeier is with the Institute for High Frequency Techniques, University of the Bundeswehr, D-8014 Neubiberg, Germany.

IEEE Log Number 9101655.

0018-9480/91/0900-1602$01.00 ©1991 IEEE

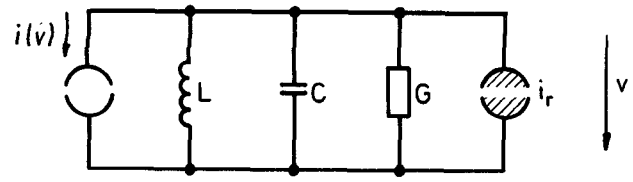


Fig. 1. Noise equivalent circuit of an oscillator.

of $G$ comprises all losses in the oscillator and the external load transformed into the circuit. The nonlinear control characteristic of the active element is described by the current source $i(v)$. The noise current source $i_r$ comprises all noise phenomena of the oscillator. The noise current $i_r$ consists of the thermal noise of the conductance $G$ and the noise contribution of the active element.

In the following derivations $i_r$ will be considered as the noise current of a fictitious equivalent noise conductance $G_e$ at room temperature $T_0$:

$$\overline{i_r^2} = 4 \cdot kT_0 \cdot G_e \cdot B. \tag{1}$$

The spectral power density of $i_r$ is then

$$W_{i_r} = \frac{\overline{i_r^2}}{B} = 4 \cdot kT_0 \cdot G_e. \tag{2}$$

The oscillator operation can be described by the differential equation (3), which can be derived from Fig. 1:

$$C \cdot \frac{dv}{dt} + G \cdot v + \frac{1}{L} \cdot \int v\,dt + i(v) + i_r(t) = 0. \tag{3}$$

First, consider the oscillator function without disturbance, i.e., $i_r(t) = 0$; the terms $C \cdot dv/dt$ and $(1/L) \int v\,dt$ cause an oscillation by periodically shifting the energy between inductance and capacitance. The oscillation is damped by the term $G \cdot v$. In the case of a steady oscillation the current source $i(v)$ which represents the active element in the circuit has to replace exactly the electrical energy which is consumed in the conductance $G$:

$$i(v) = -\alpha \cdot v + \beta \cdot v^2 + \gamma \cdot v^3 + \cdots. \tag{4}$$

The source $i(v)$ can be represented by this power series expansion, whose coefficients have to fulfill two conditions. First, the value of $\alpha$ must be larger than that of the conductance $G$ to allow a buildup of the oscillation out of the nonoscillating state. Second, the coefficients of the higher powers of $v$ have to ensure an amplitude limitation at higher voltages. Only then will a steady oscillation of the circuit with a defined voltage amplitude be possible.

Analyzing the oscillator operation including the noise current source $i_r$, the amplitude as well as the phase of the oscillator voltage shows fluctuations around the values obtained in the undisturbed case. Considering the amplitude and phase of the voltage as a function of time, (3) may be split into three separate equations. These describe the steady oscillation, the time-dependent amplitude which is responsible for the AM noise, and the time-dependent phase which is responsible for the FM noise. The equations were first solved by Mullen [3] in 1960 using a Van der Pol control characteristic (only $\alpha \neq 0$ and $\gamma \neq 0$) of the active element. The following derivation is based on a solution by Lindenmeier [5] obtained in 1974 which considers an arbitrary control characteristic and contains only values which can be measured with real oscillators.

## III. Comparison of AM and FM Noise

It is well known that the spectrum of an undisturbed oscillation with amplitude $V_0$ can be described by the Dirac function. It consists of a single spectral line at the frequency $f_0$ in which all the oscillator power is contained. In the following derivations the square of the RMS voltage, i.e., $(1/2) \cdot V_0^2$, will be considered representative for the oscillator power.

When a noise current source $i_r$ is introduced, the oscillator power is no longer concentrated at the frequency $f_0$ but rather is distributed in a frequency range around $f_0$. The carrier-to-noise ratio may be used as a measure of the widening of the spectral line. It is determined as the ratio between the total power of the carrier $(1/2) \cdot V_0^2$ and the noise power in a bandwidth $B$ at a frequency deviation $\Delta f$ from the carrier frequency $f_0$.

The carrier-to-noise ratio $a_{\mathrm{AMFM}}$ is usually given with relation to a bandwidth $B = 1$ Hz. It is

$$a_{\mathrm{AMFM}} = 10 \cdot \log \left[ \frac{(W_{\mathrm{AM}} + W_{\mathrm{FM}}) \cdot B}{\frac{1}{2} \cdot V_0^2} \right]. \tag{5}$$

In this equation $W_{\mathrm{AM}}$ and $W_{\mathrm{FM}}$ describe the spectral power densities of the amplitude and phase noise, respectively. The FM noise spectrum is, according to [6],

$$W_{\mathrm{FM}} = \frac{V_0^2}{2} \cdot \frac{1}{\pi \cdot \Delta f_{\mathrm{FM}}} \cdot \frac{1}{1 + \left( \frac{\Delta f}{\Delta f_{\mathrm{FM}}} \right)^2}. \tag{6}$$

Half of the total power in the spectrum is concentrated between the frequencies $f_0 - \Delta f_{\mathrm{FM}}$ and $f_0 + \Delta f_{\mathrm{FM}}$. Thus, $\Delta f_{\mathrm{FM}}$ is defined as

$$\int_{f_0 - \Delta f_{\mathrm{FM}}}^{f_0 + \Delta f_{\mathrm{FM}}} W_{\mathrm{FM}}(f)\,df = \frac{1}{4} V_0^2. \tag{7}$$

The quantity $\Delta f_{\mathrm{FM}}$ as a function of the equivalent circuit elements of Fig. 1 was calculated in [5]. After appropriate modification it can be rewritten as

$$\Delta f_{\mathrm{FM}} = \frac{\pi \cdot kT_0 \cdot G_e \cdot f_0^2}{P \cdot G \cdot Q_0}. \tag{8}$$

$Q_0$ is the quality factor of the resonant circuit, which is determined by the conductance $G$. $P$ is the oscillator power:

$$P = \frac{1}{2} V_0^2 \cdot G. \tag{9}$$

The AM noise spectrum may be derived from [5]

$$W_{AM} = \frac{1}{2} V_0^2 \cdot \frac{1}{\pi \cdot \Delta f_{FM}} \cdot \frac{\left(\frac{\Delta f_{FM}}{\Delta f_{AM}}\right)^2}{1 + \left(\frac{\Delta f}{\Delta f_{AM}}\right)^2} \tag{10}$$

where $\Delta f_{AM}$ is defined as the frequency deviation from $f_0$ at which $W_{AM}(f)$ has dropped to half its maximum value, i.e.,

$$W_{AM}(f_0 - \Delta f_{AM}) = W_{AM}(f_0 + \Delta f_{AM}) = \frac{W_{AM}(f_0)}{2}. \tag{11}$$

The quantity $\Delta f_{AM}$ can be obtained from [5]

$$\Delta f_{AM} = \frac{f_0}{2Q_0 \cdot \epsilon} \tag{12}$$

with

$$\epsilon = \left| \frac{dV/V_0}{dG/G} \right|. \tag{13}$$

Here $\epsilon$ describes the relative dependence of the oscillator amplitude on the load (amplitude load control). It has a strong influence on the AM noise and can have values between 0 and 1. For the (theoretical) case of a linear oscillator whose open-loop gain is exactly 1, the value of $\epsilon$ will be $\epsilon = 1$. Such an oscillator, however, will not be able to build up an oscillation; nor will it be able to sustain a stable oscillation when it is only slightly disturbed.

Oscillator measurements conducted within this work showed that a sufficiently stable oscillation, even with external disturbances and small temperature variations, was obtained up to a maximum of $\epsilon_{max} = 0.8$. Approaching the linear operation case ($\epsilon = 1$) even further leads to a dramatic decrease in oscillator stability.

With growing feedback the active element is increasingly driven into the nonlinear region and the value of $\epsilon$ becomes smaller. In this case the amplitude noise is decreased as long as other parameters such as $G_e$ and $Q_0$, which are also changed by a growing feedback, do not show adverse effects. This may happen in the case of an extremely overdriven active element, which also results in an increase in the phase noise.

Typical curves for the carrier-to-noise ratios of AM noise and FM noise are shown in Fig. 2. They belong to an oscillator with $\epsilon = 0.76$ which oscillates at $f_0 = 144$ MHz. Because of the large value of $\epsilon$, the AM noise has almost reached its maximum compared with FM noise. For increasingly nonlinear operation and, therefore, smaller $\epsilon$, the AM noise could be significantly reduced. Fig. 3 shows the contribution of the AM noise to the carrier-to-noise ratio of the described "worst case" oscillator.

A significant contribution of AM noise to the overall oscillator noise generally occurs only at relatively large frequency deviations from the carrier and, consequently, very low oscillator noise levels. Therefore, AM noise is usually of no practical importance and is neglected in the following considerations.

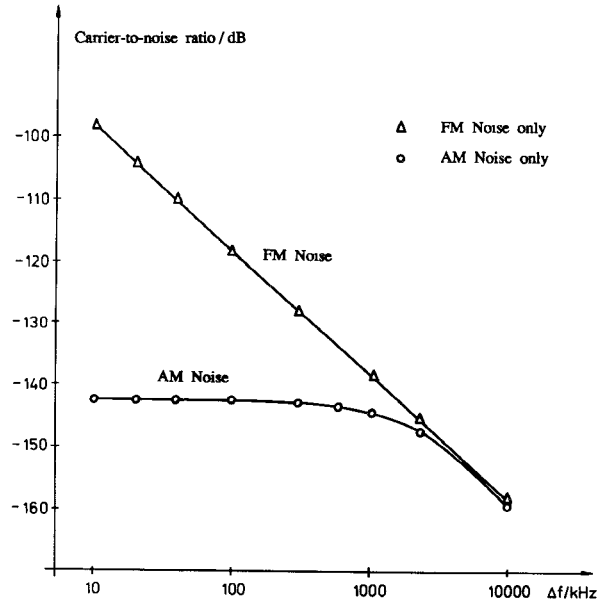


Fig. 2. Carrier-to-noise ratios of AM and FM noise.

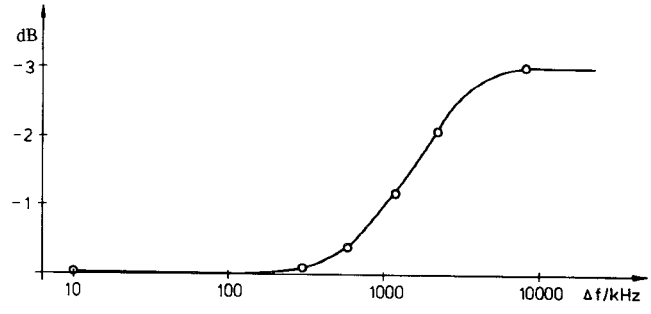


Fig. 3. Contribution of AM noise to the carrier-to-noise ratio.

By neglecting the AM noise, (5) can be simplified. With the assumption $(\Delta f/\Delta f_{FM}) \gg 1$, which is usually fulfilled, the carrier-to-noise ratio is

$$a_{FM} = 10 \cdot \log \left[ \frac{B \cdot \Delta f_{FM}}{\pi} \cdot \frac{1}{\Delta f^2} \right]. \tag{14}$$

Considering the dependence of $\Delta f_{FM}$ on the oscillator parameters (eq. (8)), the carrier-to-noise ratio can be written as

$$a_{FM} = 10 \cdot \log \left[ \frac{BkT_0 \cdot f_0^2}{P} \cdot \frac{G_e}{G} \cdot \frac{1}{Q_0^2} \cdot \frac{1}{\Delta f^2} \right]. \tag{15}$$

For very small frequency deviations $\Delta f$, the influence of the transistor's $1/f$ noise, which is up-converted into the frequency range around $f_0$, may lead to a $1/\Delta f^3$ dependence of the carrier-to-noise ratio. The effect can be minimized by a suitable choice of the active element as well as by the oscillator design. For all bipolar transistor oscillators which were investigated experimentally during this work no such influence could be detected measuring for frequency deviations $\Delta f \geq 10$ kHz.

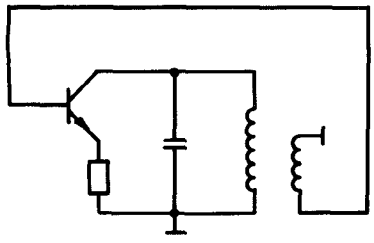

Fig. 4. AC equivalent circuit of a Meissner oscillator.

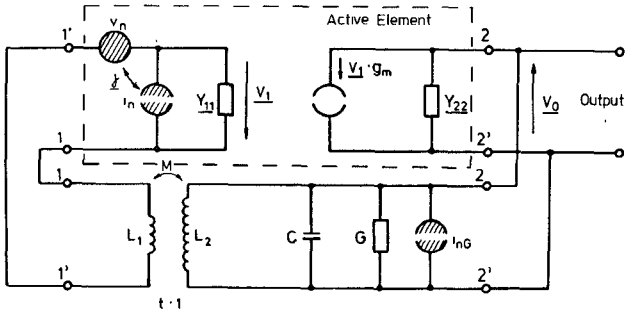


Fig. 5. Noise equivalent circuit of a Meissner oscillator.

## IV. Determination of $G_e/G$

The dependence of the signal-to-noise ratio on oscillator parameters was investigated for the Meissner oscillator (Fig. 4). The Meissner oscillator was chosen because its circuit parameters can be varied easily in the experiment. The derivation of the theory as well as the results, however, can also be applied to oscillators with other feedback mechanisms.

The noise equivalent circuit of the Meissner oscillator (Fig. 5) contains in the upper part the four-pole equivalent circuit of the active element with its short-circuit transconductance $g_m$. A possible partial coupling to the resonant circuits is already contained in the values of the transistor parameters. It is well known that any real noisy amplifier can be replaced by a noiseless four-pole with partially correlated noise sources $i_n$ and $v_n$ at its input [8]. The quantity $\gamma = \gamma_R + j \cdot \gamma_I$ is the related complex correlation coefficient.

In the lower part of Fig. 5 the parallel resonant circuit which determines the frequency of oscillation is displayed. Its inductance is at the same time the primary inductance of the transformer which feeds back a part of the oscillation voltage to the input of the active element. The no-load voltage transformation ratio, $t$, of the transformer determines the strength of the feedback.

The load conductance, $G$, can be determined out of the quality factor, $Q_0$, of the resonant circuit excluding the transistor. It contains all losses of the resonant circuit and the external load transformed into the circuit. The thermal noise of $G$ is represented by the noise current source $i_{nG}$.

The noise equivalent circuit of Fig. 5 will now be transferred into the simple noise equivalent circuit of Fig. 1, in which all noise sources are combined into one noise current source $i_r$ parallel to the resonant circuit. To do this, the noise sources of the transistor have to be transformed into a noise current source $i_{nT}$ parallel to the resonant circuit. The noise current source $i_{nG}$ of the load conductance $G$ is already situated at the appropriate location. The noise current source $i_r$ is composed of both noise sources. The equivalent noise conductance, $G_e$, in (1) is then

$$G_e = \frac{\overline{i_{nG}^2} + \overline{i_{nT}^2}}{4 \cdot kT_0 \cdot B}. \tag{16}$$

To transform the noise sources $v_n$ and $i_n$ into $i_{nT}$, the oscillator is shorted at the terminals $2-2'$. For the transformations, it is assumed that the principle of linear superposition is applicable. Then, a transformation of the noise sources independent of each other is possible. The very good agreement between theory and measurement shows that the principle of linear superposition can still be applied when the active element is overdriven as long as the biasing remains unchanged.

Both partially correlated noise sources $v_n$ and $i_n$ have to be transformed into short-circuit noise currents between the terminals $2-2'$. Each of them has to be transformed in two ways, via the active element and via the feedback circuit. For the transformation, the noise current $i_n$ is split into a part $i_{n\,\mathrm{cor}}$ that is fully correlated with $v_n$ and a part $i_{n\,\mathrm{un}}$ that is not correlated with $v_n$. Thus, a total of six transformations have to be considered. However, depending on the oscillator circuit, the resulting short-circuit noise currents may be negligible for one or more ways of transformation. For example, in this case the transformation of $v_n$ via the feedback circuit will result in a negligible noise current owing to the very small short-circuit input admittance $Y_{11}$ of the active element.

Considering further the correlation between $v_n$ and $i_{n\mathrm{cor}}$ and the fact that all short-circuit noise currents which come form the same original noise source are fully correlated with each other, a resulting noise current $i_{nT}$ can be calculated. For the oscillator circuit of Fig. 5, the equivalent noise current $i_{nT}$ of the transistor between the terminals $2-2'$ is

$$\overline{i_{nT}^2} = \overline{i_{n\,\mathrm{un}}^2} \cdot |t'|^2 + \overline{(g_m \cdot v_n + i_{n\,\mathrm{cor}} \cdot t')^2} \tag{17}$$

with

$$t' = t + g_m \left[ j\omega L_1 - j\omega M \left( \frac{M}{L_2} \right) \right]. \tag{18}$$

The additional noise figure $F_T = F - 1$ of the transistor relative to the terminals $2-2'$ can be expressed for

$T_0 = 290$ K as

$$F_T = \frac{\overline{i_{nT}^2}}{4 \cdot kT_0 \cdot G \cdot B}. \tag{19}$$

The following equation denotes the minimum additional noise figure of the noise matched active element that can be measured in an amplifier circuit:

$$F_{T\min} = \frac{\sqrt{\overline{v_n^2} \cdot \overline{i_n^2}}}{2 \cdot kT_0 \cdot B}\left(\gamma_R + \sqrt{1-\gamma_I^2}\right). \tag{20}$$

The absolute value of the optimum source admittance $\boldsymbol{Y}_{\text{opt}}$ for which the transistor exhibits its minimum noise figure is

$$Y_{\text{opt}} = |\boldsymbol{Y}_{\text{opt}}| = \sqrt{\frac{\overline{i_n^2}}{\overline{v_n^2}}}. \tag{21}$$

Inserting (17) and further using (20) and (21) for simplification, (19) becomes

$$F_T = \frac{F_{T\min}}{2 \cdot \left(\gamma_R + \sqrt{1-\gamma_I^2}\right)} \cdot \left(Y_{\text{opt}} \cdot \frac{|\boldsymbol{t}'|^2}{G} + \frac{1}{Y_{\text{opt}}} \cdot \frac{g_m^2}{G}\right). \tag{22}$$

The equivalent noise conductance $G_e$ is

$$G_e = G(1+F_T) = G \cdot F. \tag{23}$$

The noise figure $F = G_e/G$ describes the size of the complete noise source between the terminals $2-2'$ relative to the thermal noise of the resonant circuit with load only. For special cases, e.g. the theoretical case of a Meissner oscillator with an ideal transformer for feedback, the ways of transforming $v_n$, $i_{n\,\text{cor}}$, and $i_{n\,\text{un}}$ into $i_{nT}$ are reduced to one each. Then, $F$ is exactly the noise figure that the transistor with uncorrelated noise sources would show in an amplifier if it were connected to the source admittance which is present at the input of the transistor in the oscillator circuit in the non-oscillating state ($g_m = 0$).

The condition of a steady oscillation is

$$g_m \cdot t = G_{\text{tot}} \tag{24}$$

with

$$G_{\text{tot}} = G + \text{Re}\{\boldsymbol{Y}_{22}\}. \tag{25}$$

For the calculation of $G_{\text{tot}}$, the real part of the input admittance of the active element transformed into the resonant circuit would have to be added to the right-hand side of (25). Generally, however, its value is so small compared with $G$ or $\text{Re}\{\boldsymbol{Y}_{22}\}$ that it can be neglected. Using the oscillation condition, the noise figure $F$ becomes

$$F = \frac{G_e}{G} = 1 + \frac{F_{T\min}}{2 \cdot \left(\gamma_R + \sqrt{1-\gamma_I^2}\right)} \cdot \frac{G_{\text{tot}}}{G}\left(\frac{Y_{\text{opt}}}{G_{\text{tot}}} \cdot |\boldsymbol{t}'|^2 + \frac{G_{\text{tot}}}{Y_{\text{opt}}} \cdot \frac{1}{t^2}\right). \tag{26}$$

To achieve maximum signal-to-noise ratio (eq. (15)), $F$ must be minimized. This can be done by minimizing $F_{T\min}$, $G_{\text{tot}}$, and the expression in parentheses. The latter can be minimized by choosing an optimum voltage transformation ratio $t = t_{\text{opt}}$. For the Meissner oscillator, a nonnumerical solution for $t_{\text{opt}}$ can be obtained in two special cases. For a transformer with high leakage, we get

$$\omega L_1 \gg \omega M\left(\frac{M}{L_2}\right)$$

and with that

$$t_{\text{opt}} = \sqrt[4]{G_{\text{tot}}^2\left(\omega^2 L_1^2 + \frac{1}{Y_{\text{opt}}^2}\right)}. \tag{27}$$

The achievable minimum noise figure is then

$$\left(\frac{G_e}{G}\right)_{\min} = 1 + \frac{F_{T\min}}{\left(\gamma_R + \sqrt{1-\gamma_I^2}\right)} \cdot \frac{G_{\text{tot}}}{G} \cdot \sqrt{Y_{\text{opt}}^2 \cdot \omega^2 L_1^2 + 1}. \tag{28}$$

For the theoretical case of an ideal transformer without leakage, $t' = t$ and

$$t_{\text{opt}} = \sqrt{\frac{G_{\text{tot}}}{Y_{\text{opt}}}}. \tag{29}$$

The achievable minimum noise figure is

$$\left(\frac{G_e}{G}\right)_{\min} = 1 + \frac{F_{T\min}}{\left(\gamma_R + \sqrt{1-\gamma_I^2}\right)} \cdot \frac{G_{\text{tot}}}{G}. \tag{30}$$

The minimum is achieved when the conductance $G_{\text{tot}}$ is transformed via the feedback circuit into the optimum source admittance $Y_{\text{opt}}$ at the input of the transistor. Although impedances cannot be measured in an operating oscillator, the oscillator can be optimized with respect to its signal-to-noise ratio by impedance noise matching.

Using an active element with high input and output impedances compared with $G$ and uncorrelated noise sources, we get $G_{\text{tot}} = G$ and $\gamma = 0$. Then, the absolute minimum noise figure can be obtained:

$$\left(\frac{G_e}{G}\right)_{\min} = 1 + F_{T\min} = F_{\min}. \tag{31}$$

The signal-to-noise ratio of a Meissner oscillator including a transformer with a low coupling coefficient is shown in Fig. 6. The numbers along the curve denote the location of oscillators with circuit parameter sets as used in the experiment but with the assumption of a constant resonant circuit quality factor ($Q_0 = 157$) and constant amplitude ($V_0 = 9$ V). It can be seen that by an appropriate impedance noise matching the signal-to-noise ratio may be improved by as much as 30 dB.

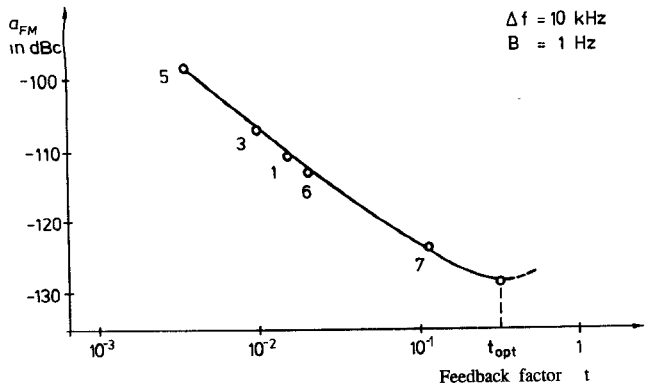


Fig. 6. Oscillator carrier-to-noise ratio for small transformer coupling coefficient. $Q_0 = \text{const.}$, $V_0 = \text{const.}$

## V. Conditions for a Low-Noise Oscillator and Their Realization

### A. Conditions

Now that $F = G_e / G$ has been determined all parameters in (15) which have an influence on the signal-to-noise ratio of the oscillator are known. Therefore, all aspects which have, according to (15), (9), (25) or (33), and (26), to be considered for the design of a low-noise oscillator can be listed:

a) Choice of a transistor with
- small noise figure $F_{T\min}$ combined with a small correlation coefficient $\gamma$,
- high output voltage $V_o$,
- high output current $I_o$,
- small output conductance $\mathrm{Re}\{Y_{22}\}$ or $G_A$,
- reasonably high input impedance.

b) Meeting an impedance condition at the input of the active element which can be reached by optimization of the feedback factor and which leads to optimum impedance noise matching.

c) High quality factor $Q_0$ of the resonant circuit.

d) High transformer coupling coefficient in the case of a Meissner oscillator.

Depending on the oscillator type, it may be possible that not all the conditions a)–d) can be met at the same time. In such cases the best signal-to-noise ratio can be achieved by optimization of the interdependent parameters.

### B. Realization of an Optimum Active Element

Considering the criteria for the choice of an optimum active element it was not possible to find a single transistor that meets all requirements. Instead, it is much more promising to combine the active element out of two or more suitable transistors. Required is a low-noise input stage with reasonably high input impedance and a final stage with high output power capability and a high output impedance. One active element that can fulfill these requirements is shown in Fig. 7.

The final stage consists of a bipolar transistor with high output power capability in a common-base configuration. Compared with other configurations the transistor in the common-base configuration shows the highest output impedance for almost linear operation as well as in saturation.

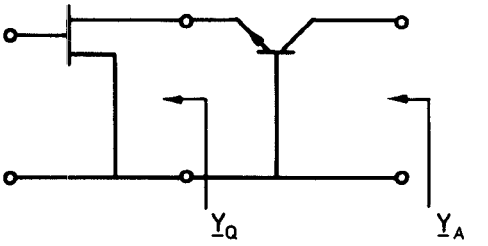


Fig. 7. Optimum active element.

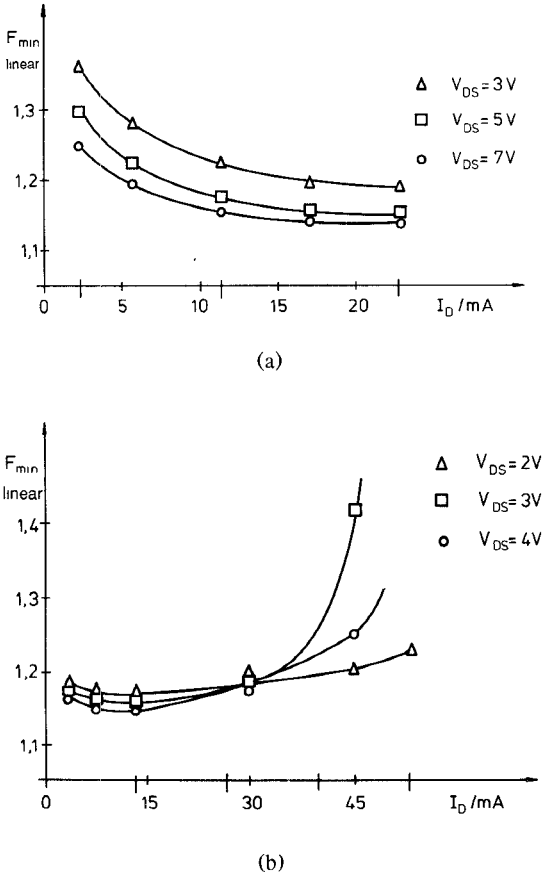


Fig. 8. Minimum noise figure of GaAs FET's at $f = 100$ MHz: (a) GAT 1/010; (b) NE 244.

For the input stage, a field-effect transistor with a high input impedance and a low noise figure is used. Especially with GaAs FET's even at frequencies in the VHF range small amplifier noise figures can be obtained, e.g. at 100 MHz typically 0.6 dB or less, which, however, is combined with correlation coefficients $\gamma \approx j \cdot 0.85$ [7].

On the other hand there are also limitations to the use of a GaAs FET in oscillators which depend on its noise properties. One of those properties is the strong dependence of the minimum noise figure of the GaAs FET on its bias. In Fig. 8 this dependence of $F_{\min}$ is displayed in a

linear scale (not in dB!) for two GaAs FET's which have often been used in recent years. The qualitative dependence of the minimum noise figure on bias shown in Fig. 8(a) is typical for low-frequency JFET's and a few HF GaAs FET's such as the GAT 1/010. All microwave GaAs FET's used today show a dependence of the minimum noise figure on bias that qualitatively resembles the graphs in Fig. 8(b).

It is obvious that a small minimum noise figure is reached only in a small bias range. Especially for the transistor type of Fig. 8(b) the minimum noise figure in other parts of the bias characteristics can be much larger and surpass even values of $F_{\min} = 10$. The characteristic dependence of the minimum noise figure of microwave GaAs FET's on biasing can also explain why the design of low-noise oscillators with only one microwave GaAs FET is hardly possible even though the active element has a small noise figure for small-signal amplifier operation. That is, when using only one microwave GaAs FET as the active element in an oscillator because of the need for a nonlinear characteristic large-signal operation cannot be avoided. In this way regions with large noise figures are also touched and the advantage of a small noise figure in a small bias range is more than compensated. Thus, in the case of a dual-stage active element as in Fig. 7, a possible GaAs FET input stage has to operate under small-signal conditions in the bias range best suited for minimum noise figure. In this case the small amplifier noise of a GaAs FET can also be used to minimize oscillator noise.

Another problem encountered with the use of GaAs FET's in oscillators is a result of their relatively large $1/f$ noise. This can be up-converted into the frequency range around $f_0$ and at very small frequency deviations from the carrier it can lead to a large deterioration of the signal-to-noise ratio. Even today, the quantity of the $1/f$ noise can hardly be predicted by theory. Also noise measurements show large differences in the quantity of the $1/f$ noise for different GaAs FET's [7]. Since a nonlinear transfer characteristic is required for up-conversion of the $1/f$ noise, its influence on the signal-to-noise ratio of the oscillator may be kept small by a proper choice of the GaAs FET and also by a nearly linear operation of the GaAs FET in the oscillator.

Theoretically, the oscillator signal-to-noise ratio can be improved using a two-stage active element as in Fig. 7 (input stage with GAT 1/010) by up to 15 dB relative to a single bipolar transistor oscillator. Obviously, as semiconductor technology advances, other solutions for the active element which fulfill the conditions in subsection V-A may become even more attractive.

### C. Partial Coupling of the Active Element to the Resonant Circuit

The oscillator signal-to-noise ratio (eq. (15)) is related to the power of the carrier:

$$P = \frac{1}{2} V_o^2 \cdot G. \tag{32}$$

Therefore, it is proposed to use an active element with high output power capability. However, the capability provided must also be used to its full extent. The high quality factor of the resonant circuit required and the consequent small conductance $G$ mean that a large voltage amplitude $V_o$ is necessary.

Connecting the active element directly to the terminals of the resonant circuit in the case of a large load impedance leads to a limitation of the voltage amplitude by the maximum voltage of the final amplifier stage without taking full advantage of its output power capability. By a partial coupling of the active element to the resonant circuit, however, it is possible to use its full output power capability to generate oscillator power. In Fig. 9 the output part of the active element is replaced by an equivalent circuit with a current source $I_o$ and an output admittance $Y_A$ which is coupled only to a part of the resonant circuit's inductance. The coupling factor is calculated as the relation between $L_a$ and the total inductance: $L = L_a + L_b$. In Fig. 10 the oscillator voltage amplitude $V$ is shown as a function of the coupling factor $L_a/L$ for the bipolar transistor BFW 92. The graph is related to the maximum voltage and current capability of the transistor and the given conductance $G = 60\ \mu$S. The shape of the curve, however, will also be similar for other components.

Besides an enlargement of the oscillator voltage amplitude, the partial coupling of the active element to the resonant circuit reduces the effective output admittance of the active element on the resonant circuit. The value of $G_{\text{tot}}$ which has influence on the signal-to-noise ratio via $G_e$ in (15) is then

$$G_{\text{tot}} = G + \left(\frac{L_a}{L}\right)^2 \cdot G_A. \tag{33}$$

In this case the improvement of the signal-to-noise ratio by appropriate partial coupling is 14 dB, compared with full coupling to the resonant circuit. For final stage transistors with higher current limitations the potential improvement by partial coupling may be considerably larger.

## VI. Optimum Oscillator Design and Expected Results

Based on the previous considerations, a theoretical approach to an optimally designed oscillator is made. The limits of the achievable carrier-to-noise ratio are predicted using performance parameters of currently available components. Results are shown for an optimally designed Meissner oscillator whose high-frequency equivalent circuit is shown in Fig. 11.

When coupling the external load to the magnetic field of the resonant circuit's inductance the signal-to-noise ratio in the load at a large frequency deviation from the carrier is limited to a maximum value. That value is determined by the ratio of the power output $P_{\text{out}}$ consumed in the load to the thermal noise power generated by the load itself.

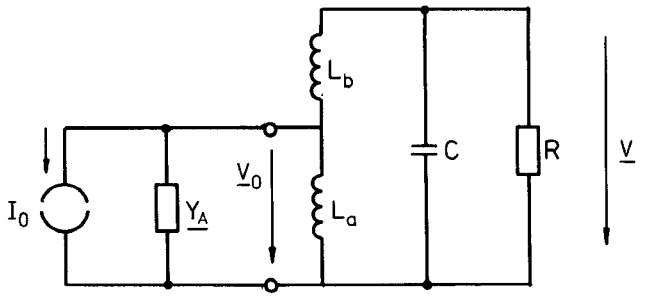


Fig. 9. Partial coupling to the resonant circuit.

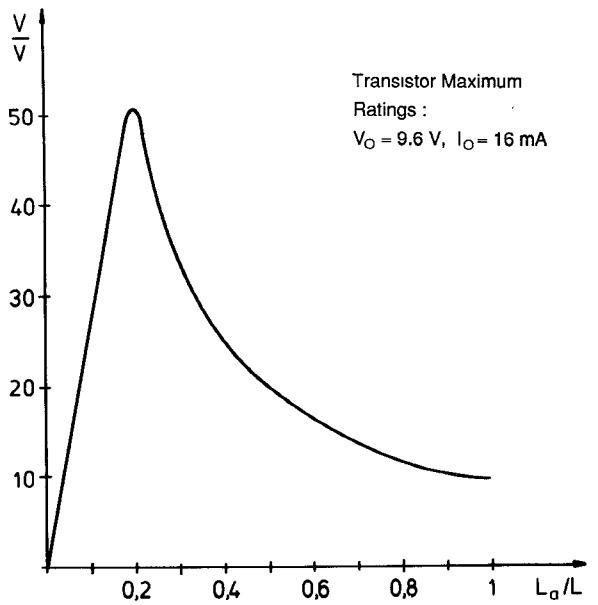


Fig. 10. Oscillator voltage amplitude as a function of the partial coupling factor to the resonant circuit.

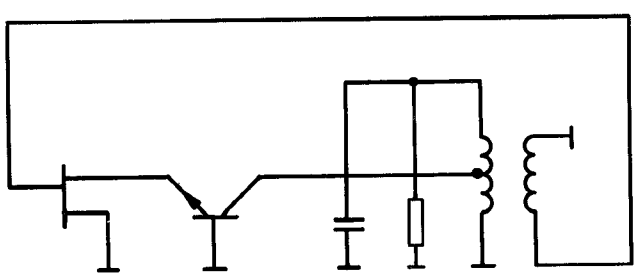

Fig. 11. AC equivalent circuit of an optimally designed Meissner oscillator.

Varying the power output $P_{out}$ to the load leads to the curves in Fig. 12, which are based on an oscillator with $Q_{0max} = 300$ for $P_{out} = -24$ dBm and $V_o = 35$ V. Its active element is directly connected to the terminals of the resonant circuit (no optimum partial coupling). The feedback factor was optimized for a lossy feedback circuit.

In this context it has to be considered that AM and FM noise contribute equally to the thermal noise floor. Therefore, in Fig. 12 the contribution of the AM noise is included. Fig. 12 shows that far away from the carrier the carrier-to-noise ratio is determined only by the power

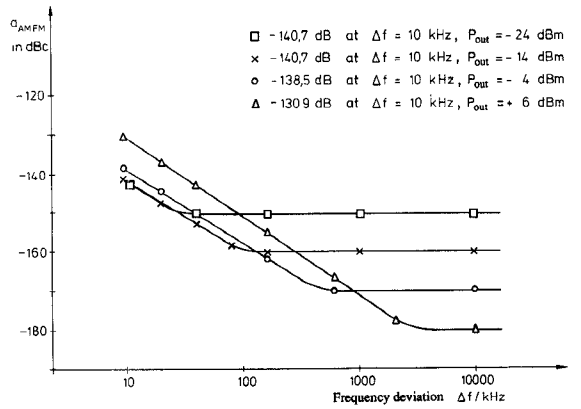


Fig. 12. Carrier-to-noise ratio as a function of the power output, $P_{out}$, to the external load.

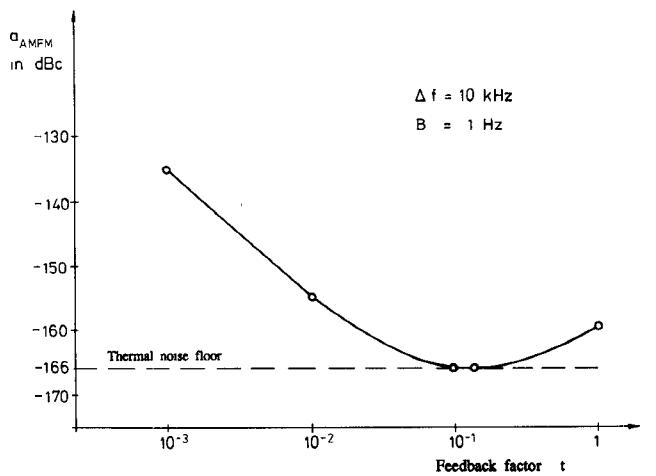


Fig. 13. Carrier-to-noise ratio of an optimally designed oscillator with $Q_o = 300$, $V_o = 35$ V, $I_o = 60$ mA, $P_{out} = -8$ dBm.

output $P_{out}$ to the load. Therefore, reducing $P_{out}$ to improve the signal-to-noise ratio near the carrier makes sense only as long as a considerable improvement of the quality factor and thereby of the signal-to-noise ratio can be obtained.

Let us now assume a lossless feedback circuit and optimize $P_{out}$ and the feedback factor $t$ at the same time. Then, for a 150 MHz oscillator with available transistors (final stage $V_o = 35$ V, $I_o = 60$ mA) and an $LC$ resonant circuit with $Q_0 = 300$, a signal-to-noise ratio of 166 dBc for a frequency deviation from the carrier of 10 kHz can be reached in a 50 Ω external load (Fig. 13). When noise matching is achieved ($t = t_{opt}$) the noise sources of the active element contribute less than 20% to the total oscillator noise power. For an external load with a far higher impedance or in the case of coupling the external load to the resonant circuit with an ideal transformer, a still better signal-to-noise ratio could be achieved. Its absolute maximum is determined by the ratio of the available oscillator power to the thermal noise power in bandwidth $B$ multiplied by the noise figure of the active

element. Using the same components as for the oscillator in Fig. 13, this leads to a theoretical limit for the signal-to-noise ratio of more than 190 dBc. A further increase of that limit is dependent only on the output power capability of the final stage transistor, which is determined by semiconductor technology.

## VII. Conclusions

An oscillator noise theory has been presented which makes it possible to predict the carrier-to-noise ratio of a real transistor oscillator on the basis of parameters of the active element and the oscillator circuit which can be easily measured. Based on this theory, conditions for the noise minimization of transistor oscillators have been derived and applied to oscillators with real components. The selection of, preferably, a multistage amplifying element with a low minimum noise figure, the adjustment of the optimum source impedance for that active element, and driving it to its maximum output power have been shown to be important conditions for reaching low oscillator noise. An improvement of the carrier-to-noise ratio by more than 50 dB compared with a nonoptimized oscillator may thus be obtained.

## References

[1] B. Van der Pol, "A theory of the amplitude of free and forced triode vibrations," *Radio Review* vol. 11, pp. 701–710, 1920; vol. 12, pp. 754–762.

[2] A. Spälti, "Der Einfluss des thermischen Widerstandsrauschens und des Schroteffekts auf die Störmodulation von Oszillatoren," *Bulletin des Schweizer Elektrotechnischen Vereins*, vol. 13, pp. 419–427, June 1948.

[3] J. A. Mullen, "Background noise in nonlinear oscillators," *Proc. IRE*, vol. 8, pp. 1467–1473, 1960.

[4] D. B. Leeson, "A simple model of feedback oscillator noise spectrum," *Proc. IEEE*, vol. 2, pp. 329–330, 1966.

[5] H. Lindenmeier, "Rauschspektrum von Transistoroszillatoren mit beliebiger Nichtlinearität," unpublished report, 1974.

[6] H. Lindenmeier, "Noise matching techniques in transistor oscillators," in *Proc. IEEE Symp. Circuits Syst.* (Houston), Apr. 1980, pp. 1052–1055.

[7] G. Braun, "Impedanz-Rauschanpassung in Transistoroszillatoren zur Optimierung des Rauschabstandes," doctor's thesis, University of the Bundeswehr Munich, Germany, July 1985.

[8] H. Rothe and W. Dahlke, "Theorie rauschender Vierpole," *Arch. Elek. Übertragung.*, vol. 9, pp. 117–121, 1955, "Theory of noisy fourpoles," *Proc. IRE*, pp. 811–818, June 1956.

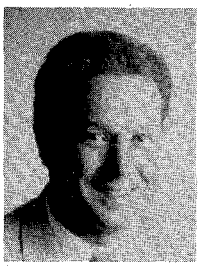

**Günter Braun** (M'87) was born in Lüdersdorf, Germany, in 1949. He received the M.S. degree in electronic engineering from the Technical University, Munich, in 1974, and the Ph.D. degree from the University of the Bundeswehr, Munich, in 1985.

From 1974 to 1982 he was with the Siemens Communications Division, Munich, where he worked on the development of microwave radio systems. From 1983 to 1986 he was with the University of the Bundeswehr, Munich, where he lectured on high-frequency electronics and supervised the production of computer films dealing with electromagnetic waves. His research interests included the noise optimization of HF oscillators and disintegration methods for bladder, ureter, and kidney stones. In 1986, Dr. Braun joined the MBB Space Systems Division, Munich, where he has been engaged in the development of antennas and measurement equipment up to 220 GHz, the design of spaceborne radar antennas for earth observation and planetary missions, and the payload design for a mobile satellite communication system. He is currently project manager for spaceborne active phased array antennas and miniaturized microwave circuits including MMIC's.

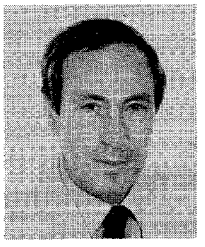

**Heinz Lindenmeier** (M'83) received the M.S. degree in communication engineering and the Ph.D. (in 1967) from Munich Technical University, FRG. He obtained his qualification as a university lecturer in 1971.

Since 1978 he has been a Professor at the University of the Bundeswehr, Munich, and head of the Institute of High Frequency Electronics.

Dr. Lindenmeier is member of URSI. His research interests include active antennas and mobile communications.